Supporting Information

Cobalt Phosphides Nanowires with Adjustable Iridium Realizing Excellent Bifunctional Activity for Acidic Water Splitting

Yun Tong[a,b] *and Pengzuo Chen*[b*]

[a] Department of Chemistry, Key Laboratory of Surface & Interface Science of Polymer Materials of Zhejiang Province, Zhejiang Sci-Tech University, Hangzhou 310018, China

[b] Institute of Chemical Sciences and Engineering, École Polytechnique Fedérale de Lausanne (EPFL), 1015 Lausanne, Switzerland.

Correspondence and requests for materials should be addressed to P. Z. Chen (E-mail: pzchen@mail.ustc.edu.cn)

Table of contents

Figure S1 The a) XRD pattern and b) SEM image of Co-based precursor on carbon cloth substrate. 4

Figure S2 The a) XRD pattern and b) SEM image of CoP-CC product. 4

Figure S3 The a) XRD pattern and b) SEM image of Ir_3-CoP-CC product. 5

Figure S4 The TEM images of as-prepared a) CoP, b) Ir_1-CoP, c) Ir_2-CoP and d) Ir_4-CoP samples. 5

Figure S5 The additional TEM images of as-prepared Ir_3-CoP products. 6

Figure S6 The EDS spectrum of Ir_3-CoP sample. 6

Figure S7 The element mapping images of CoP sample. 7

Figure S8 The element mapping images of Ir_1-CoP sample. 8

Figure S9 The element mapping images of Ir_2-CoP sample. 9

Figure S10 The element mapping images of Ir_4-CoP sample. 9

Figure S11 The XPS spectra of Ir_1-CoP/CC, a) Co 2p, b) Ir 4f and c) P 2p. 10

Figure S12 The XPS spectra of Ir_2-CoP/CC, a) Co 2p, b) Ir 4f and c) P 2p. 11

Figure S13 The XPS spectra of Ir_4-CoP/CC, a) Co 2p, b) Ir 4f and c) P 2p. 12

Figure S14 Chronoamperometric response of Ir_3-CoP-CC catalyst at -0.1 V vs. RHE for HER. 13

Figure S15 The HER performance normalized by the amount of Ir for all catalysts. 13

Figure S16 Electrochemical CV of a) CoP-CC, b) Ir_1-CoP-CC, c) Ir_2-CoP-CC and d) Ir_4-CoP-CC catalysts for HER at scanning rates from 20 to 100 mV/s. 14

Figure S17 The N_2 adsorption/desorption isotherms of Co-precursor, Ir_3 doped Co-precursor and Ir_3-CoP samples. 15

Figure S18 The OER LSV curves of Ir doped CoP/CC catalysts synthesized by different usage of $IrCl_3$. 16

Figure S19 The ECSA normalized performance for OER. 16

Figure S20 Chronopotentiometric test of Ir_3-CoP/CC catalyst at 10 mA cm^{-2} for OER in acidic medium. 17

Figure S21 The polarization curves with and without IR correction of Ir_4-CoP/CC catalyst for a) HER and b) OER. 17

Figure S22 a, d) The XRD patterns, b, e) TEM images and c, f) element mapping images of Ir_3-CoP/CC catalyst after HER and OER tests. 18

Table S1. The content of each elements for all prepared catalysts. 18

Table S2. The comparison of HER activity for other state-of-the-art Co-based electrocatalysts. 19

Table S3. The comparison of OER performance for other state-of-the-art Co-based electrocatalysts. 20

Table S4. Comparison of overall water splitting activity data for bifunctional electrocatalysts. 21

Reference 22

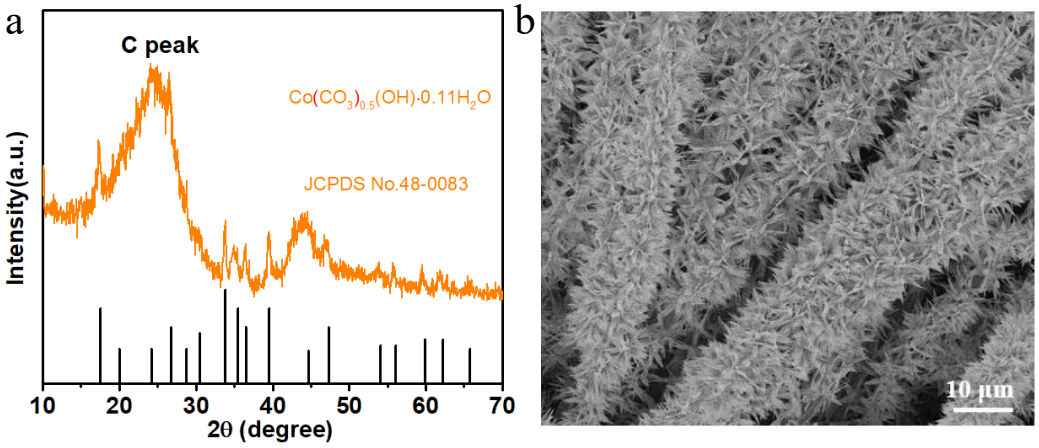

Figure S1 The a) XRD pattern and b) SEM image of Co-based precursor on carbon cloth substrate.

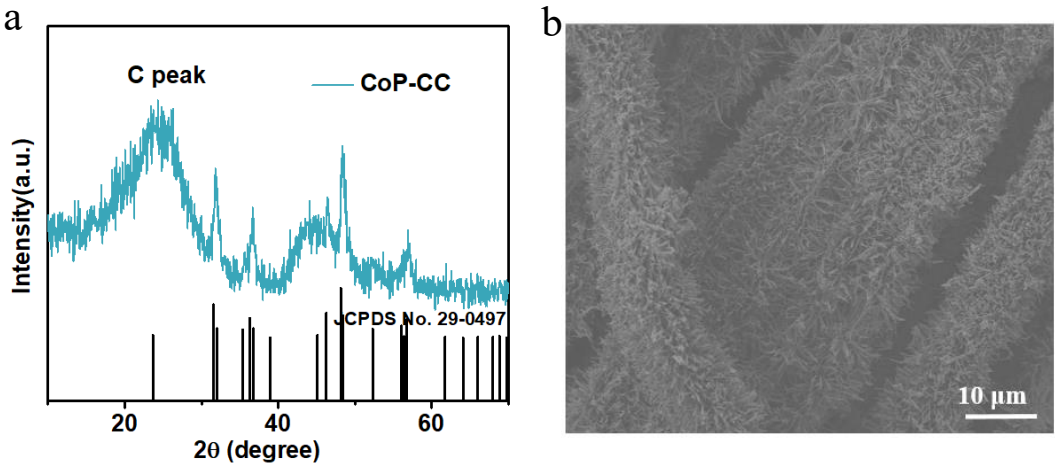

Figure S2 The a) XRD pattern and b) SEM image of CoP-CC product.

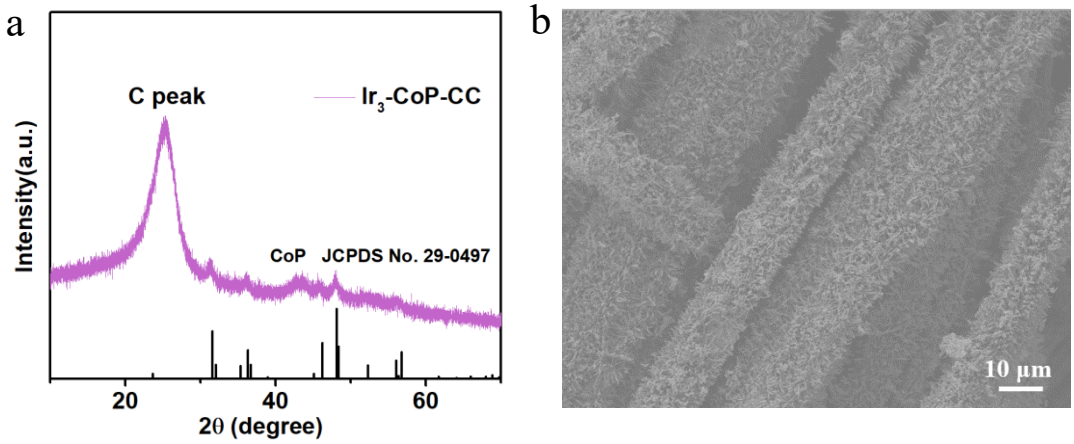

Figure S3 The a) XRD pattern and b) SEM image of Ir_3-CoP-CC product.

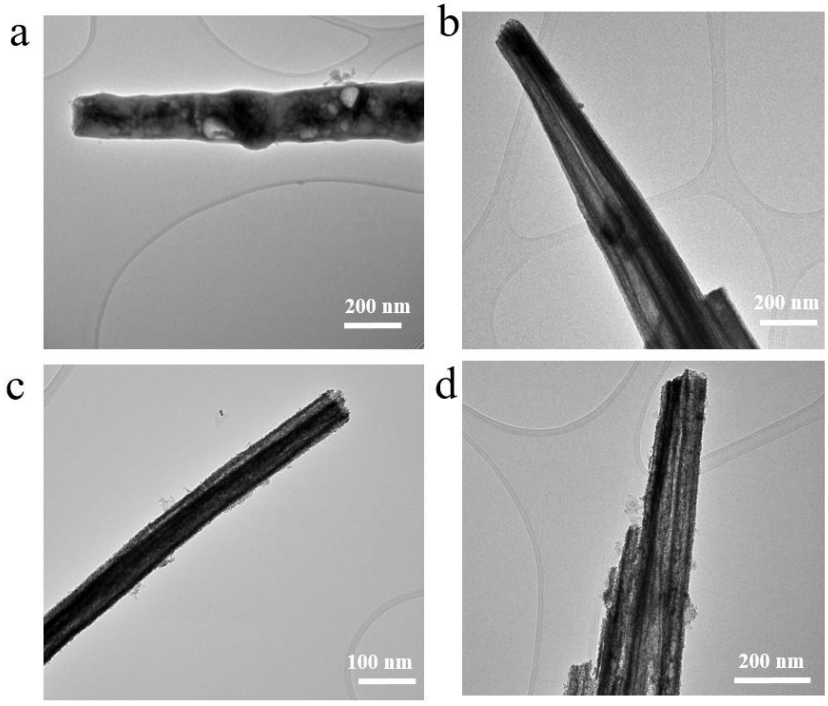

Figure S4 The TEM images of as-prepared a) CoP, b) Ir_1-CoP, c) Ir_2-CoP and d) Ir_4-CoP samples.

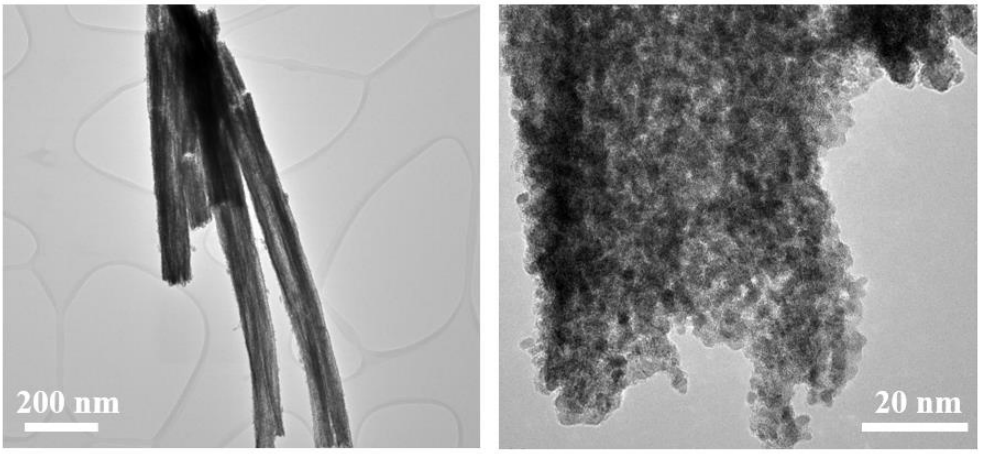

Figure S5 The additional TEM images of as-prepared Ir_3-CoP products.

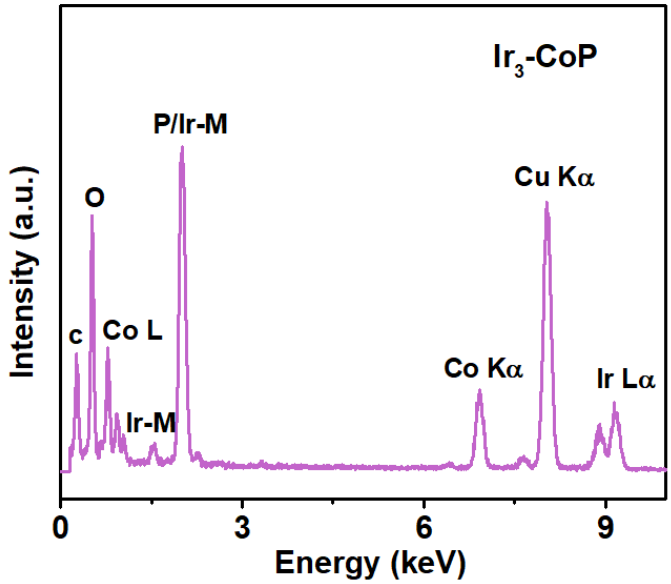

Figure S6 The EDS spectrum of Ir_3-CoP sample.

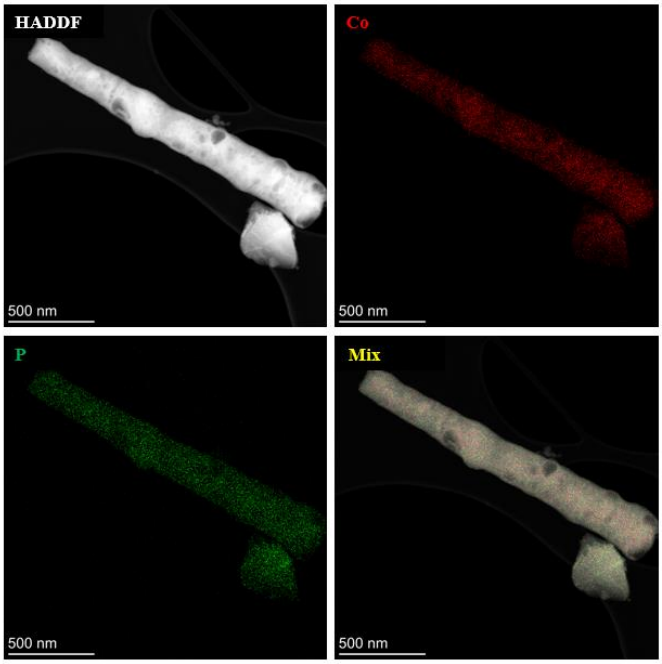

Figure S7 The element mapping images of CoP sample.

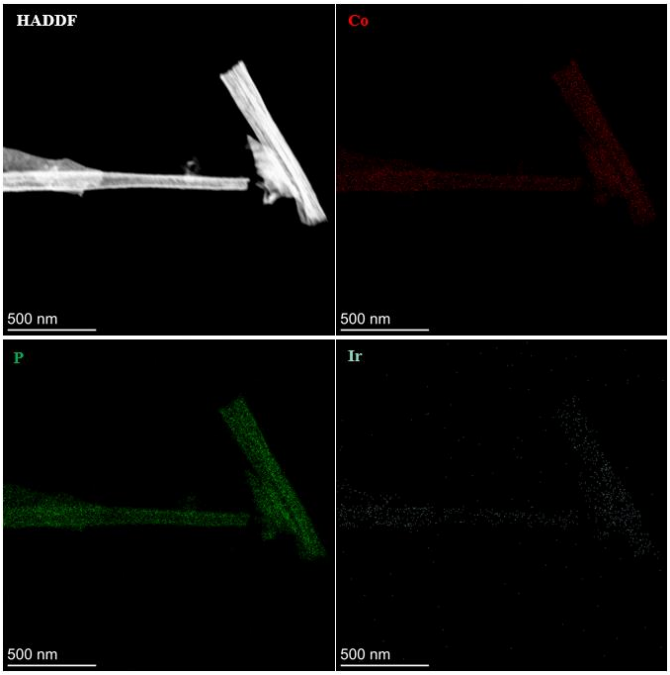

Figure S8 The element mapping images of Ir_1-CoP sample.

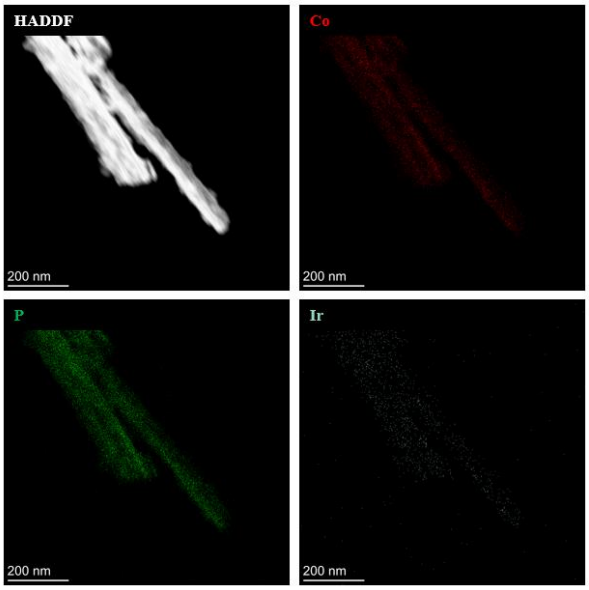

Figure S9 The element mapping images of Ir_2-CoP sample.

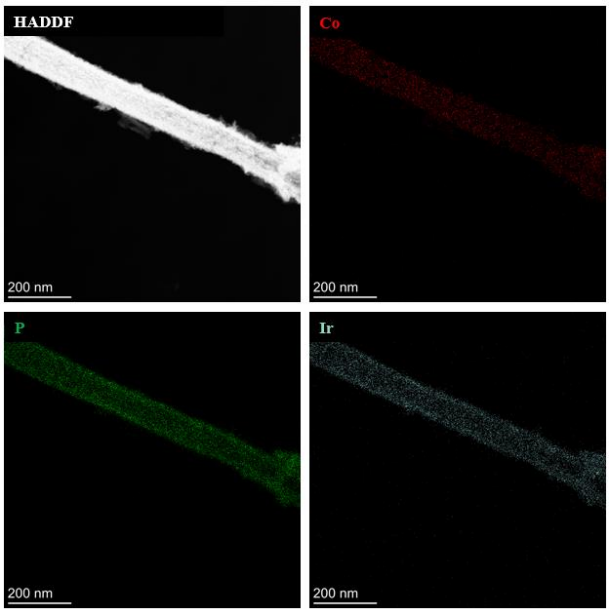

Figure S10 The element mapping images of Ir_4-CoP sample.

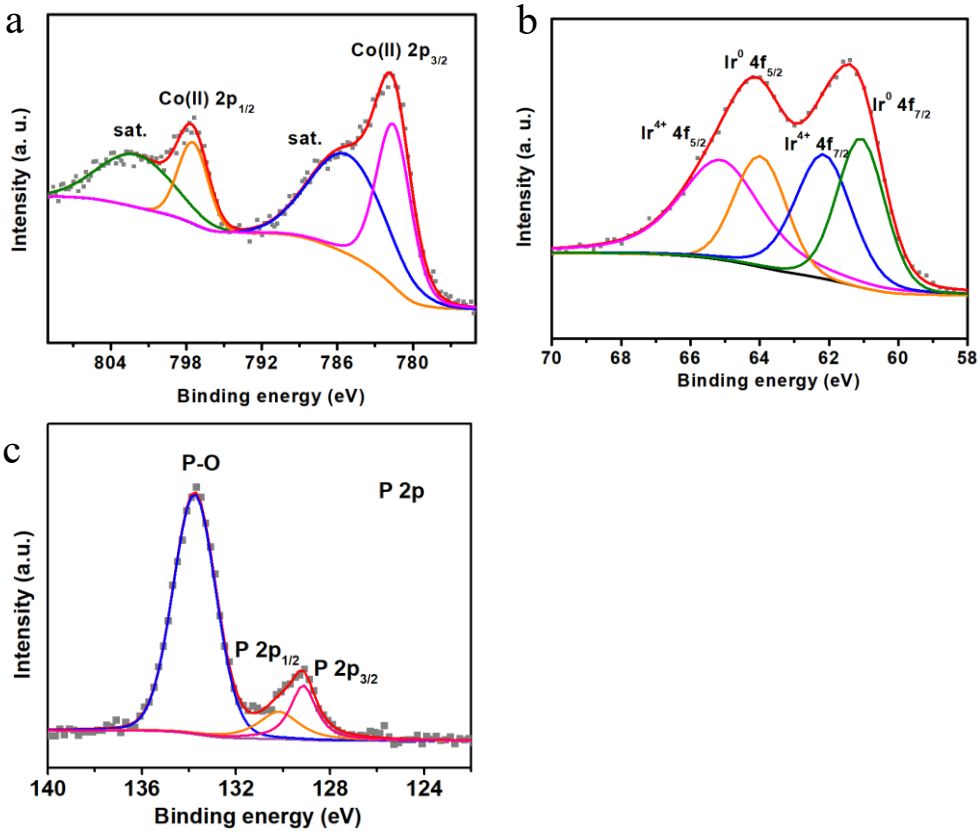

Figure S11 The XPS spectra of Ir_1-CoP/CC, a) Co 2p, b) Ir 4f and c) P 2p.

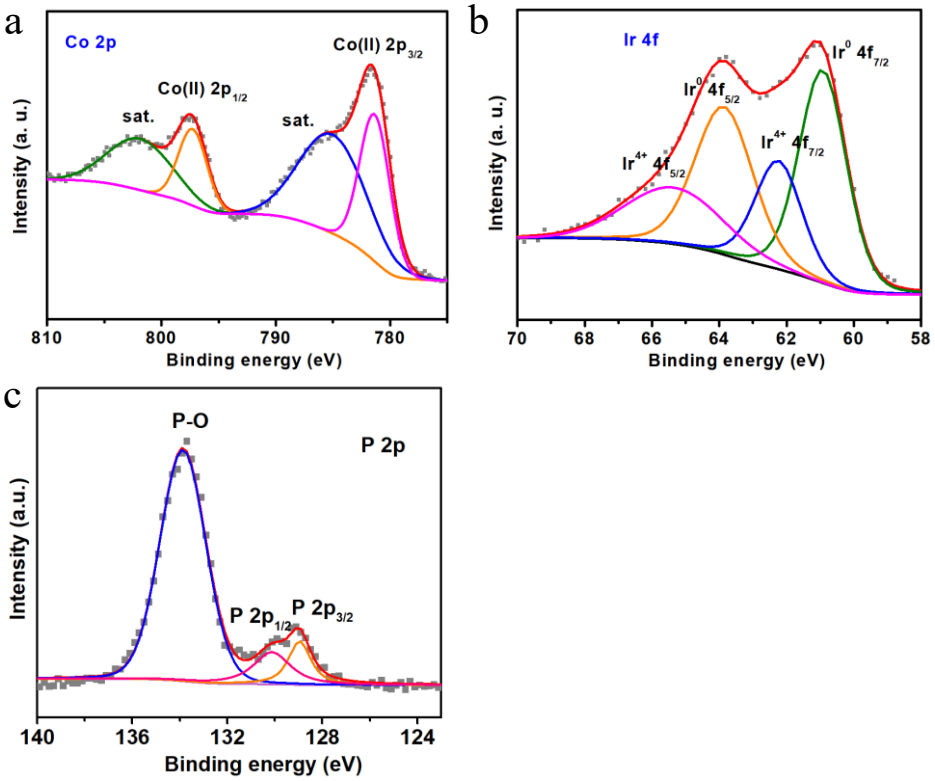

Figure S12 The XPS spectra of Ir_2-CoP/CC, a) Co 2p, b) Ir 4f and c) P 2p.

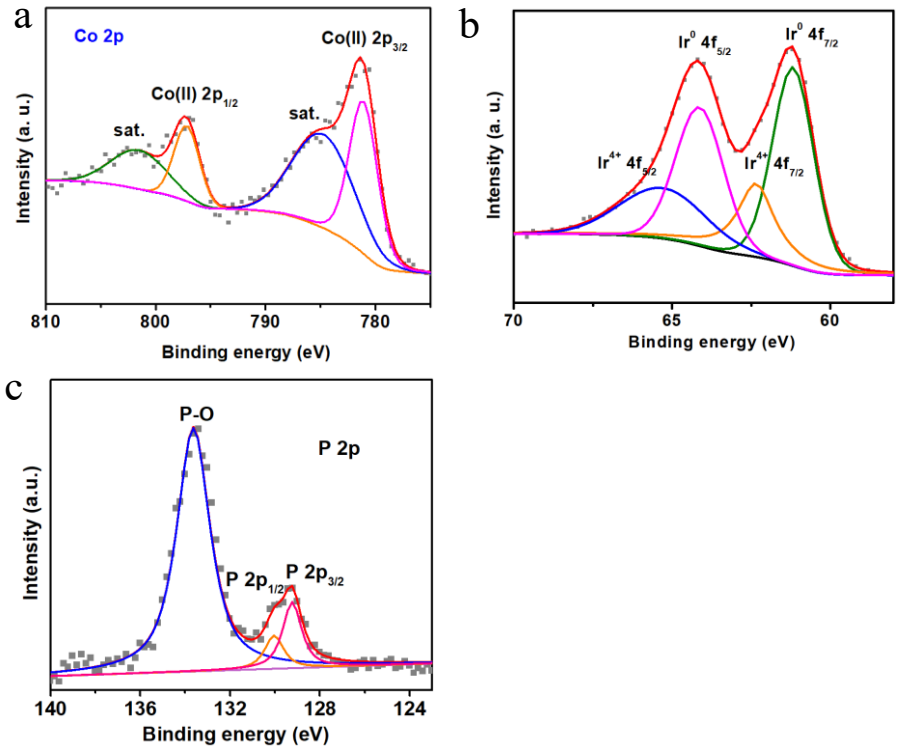

Figure S13 The XPS spectra of Ir_4-CoP/CC, a) Co 2p, b) Ir 4f and c) P 2p.

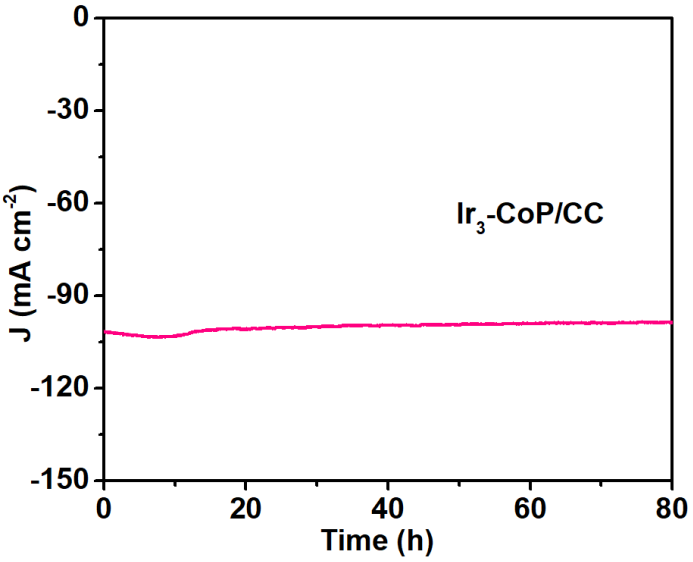

Figure S14 Chronoamperometric response of Ir_3-CoP-CC catalyst at -0.1 V vs. RHE for HER.

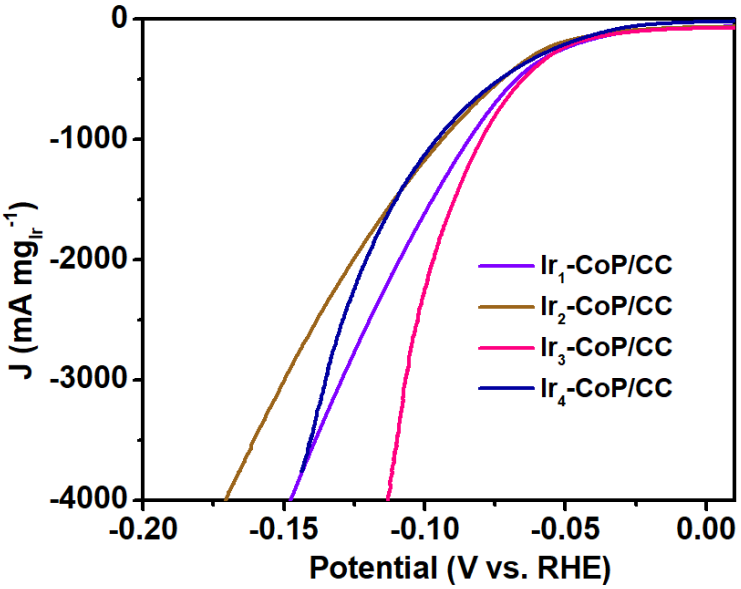

Figure S15 The HER performance normalized by the amount of Ir for all catalysts.

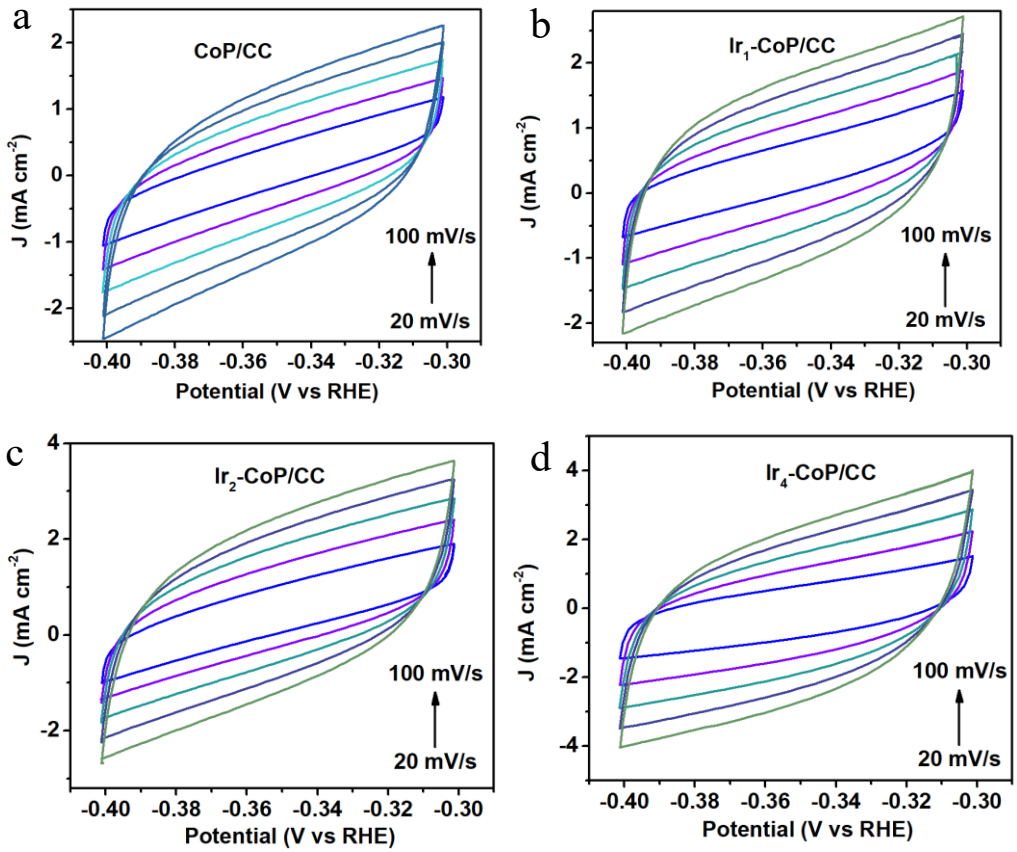

Figure S16 Electrochemical CV of a) CoP-CC, b) Ir_1-CoP-CC, c) Ir_2-CoP-CC and d) Ir_4-CoP-CC catalysts for HER at scanning rates from 20 to 100 mV/s.

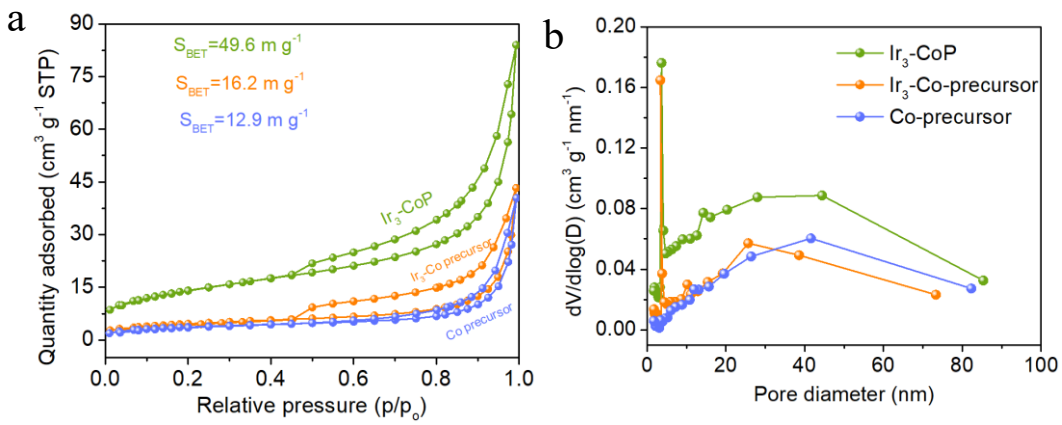

Figure S17 The N_2 adsorption/desorption isotherms of Co-precursor, Ir_3 doped Co-precursor and Ir_3-CoP samples.

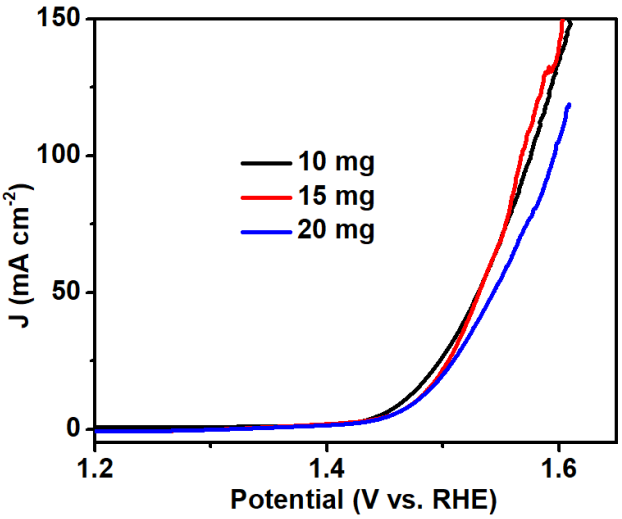

Figure S18 The OER LSV curves of Ir doped CoP/CC catalysts synthesized by different usage of $IrCl_3$.

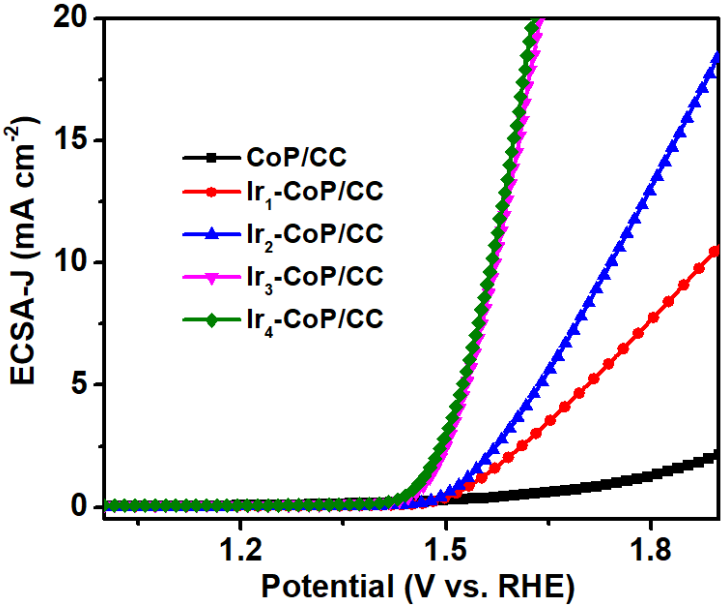

Figure S19 The ECSA normalized performance for OER.

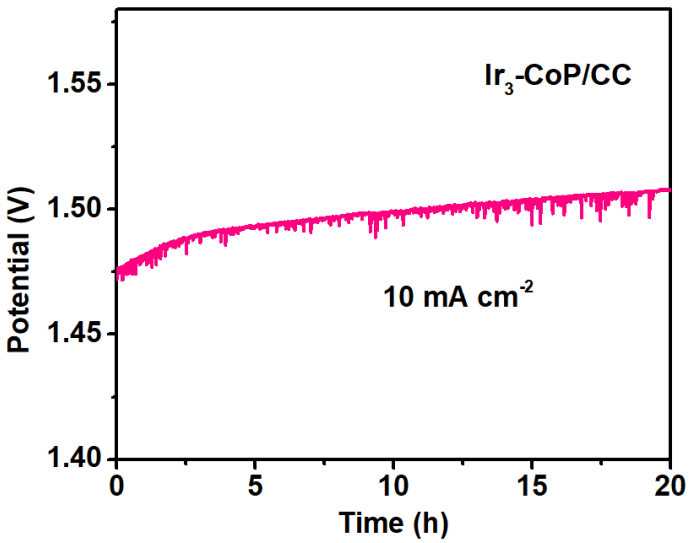

Figure S20 Chronopotentiometric test of Ir_3-CoP/CC catalyst at 10 mA cm^{-2} for OER in acidic medium.

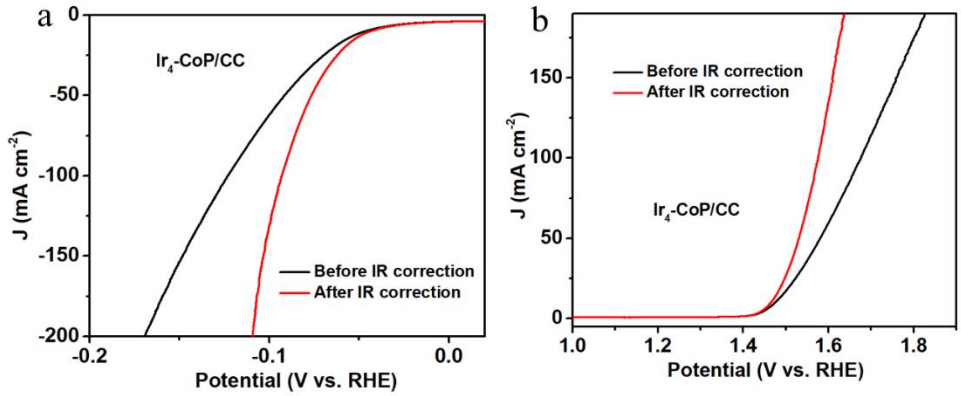

Figure S21 The polarization curves with and without IR correction of Ir_4-CoP/CC catalyst for a) HER and b) OER.

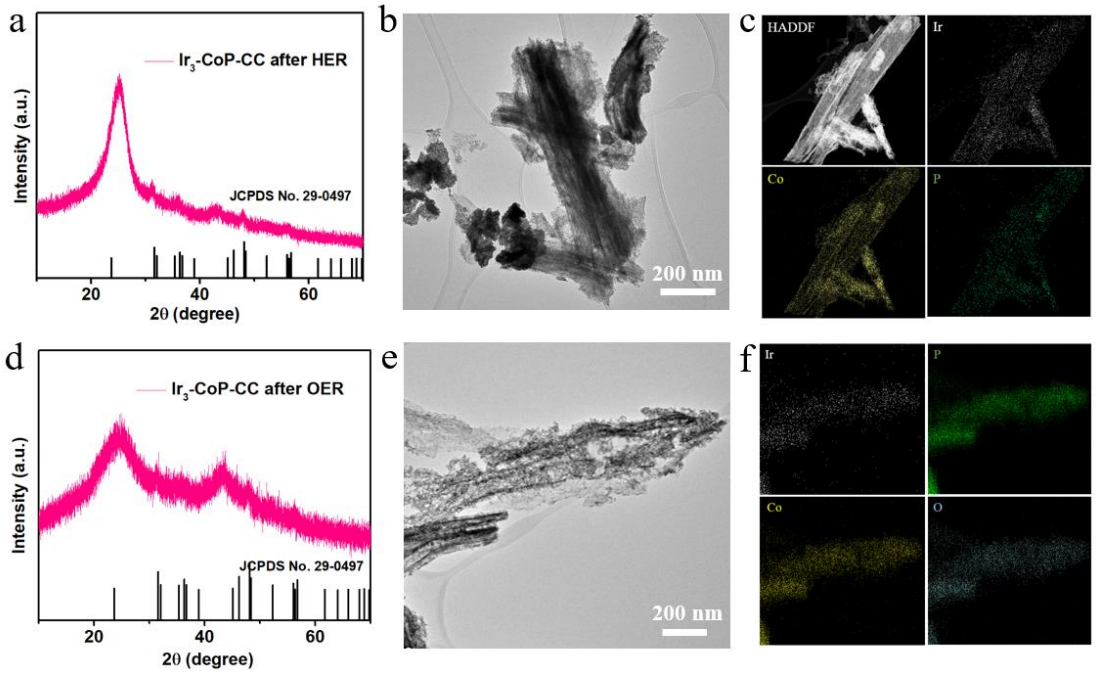

Figure S22 a, d) The XRD patterns, b, e) TEM images and c, f) element mapping images of Ir_3-CoP/CC catalyst after HER and OER tests.

Table S1. The content of each elements for all prepared catalysts.

Catalysts	**Elements (EDS)**			**ICP**
	Co	P	Ir	Ir
CoP-CC	48.7	51.3	0	0
Ir_1-CoP-CC	48.1	51.1	0.8	0.93
Ir_2-CoP-CC	47.3	50.8	1.9	2.01
Ir_3-CoP-CC	46.5	49.0	4.5	4.74
Ir_4-CoP-CC	43.8	49.6	6.6	7.02

Table S2. The comparison of HER activity for other state-of-the-art Co-based electrocatalysts.

Catalysts	η_{10} (mV)	Tafel slope (mV dec^{-1})	Electrolyte	References
Ir_3-CoP-CC	41	48	0.5 M H_2SO_4	This work
Ir_4-CoP-CC	38	69		
Co-P@PC	72	49	0.5 M H_2SO_4	[1]
CoP HNS/CF	69	/	0.5 M H_2SO_4	[2]
CoP NFs	122	54.8	0.5 M H_2SO_4	[3]
Cu-Co-P film	262	59	0.5 M H_2SO_4	[4]
Ce-doped CoP	54	59.3	0.5 M H_2SO_4	[5]
Co_2P@ NPG	103	58	0.5 M H_2SO_4	[6]
$Ni_{1.5}Co_{1.4}P$@Ru	49	49	0.5 M H_2SO_4	[7]
Ru_1CoP/CDs	51	52.3	0.5 M H_2SO_4	[8]
W-CoP	63	56	0.5 M H_2SO_4	[9]
$Fe_{0.5}Co_{0.5}P$/CC	37	30	0.5 M H_2SO_4	[10]
CoP/NPC/TF	91	54	0.5 M H_2SO_4	[11]
Pt /np-$Co_{0.85}Se$	55	35	0.5 M H_2SO_4	[12]
V-CoP/CC	47	54.9	0.5 M H_2SO_4	[13]
$Ni_{0.5}Co_{1.5}P$@ NC NA/NF	41	53.9	0.5 M H_2SO_4	[14]
CoP/Co_2P@NC NA/NF	55	55.6	0.5 M H_2SO_4	
$Ni_{1.5}Co_{0.5}P$@NC NA/NF	63	58.2	0.5 M H_2SO_4	

Table S3. The comparison of OER performance for other state-of-the-art Co-based electrocatalysts.

Catalysts	η_{10} (mV)	Tafel slope (mV dec^{-1})	Electrolyte	References
Ir_3-CoP-CC	242	71	0.5 M H_2SO_4	This work
Ir_4-CoP-CC	237	70		
$Y_2[Ru_{1.6}Y_{0.4}]O_{7-\delta}$	245	37	0.1 M $HClO_4$	[15]
Ru-N-C	267	52.6	0.5 M H_2SO_4	[16]
$R_2Ir_2O_7$	290	/	0.1 M $HClO_4$	[17]
Ir/GF	290	46	0.5 M H_2SO_4	[18]
Ir-$NiCo_2O_4$ NSs	240	60	0.5 M H_2SO_4	[19]
N-WC nanoarray	245	/	0.5 M H_2SO_4	[20]
Co-MoS_2-0.5	60	64.7	0.5 M H_2SO_4	[21]
$SrTiO_3$-$SrIrO_3$	265	50	0.5 M H_2SO_4	[22]
AuCu@IrNi	355	56	0.5 M H_2SO_4	[23]
Ir_3Ni_2/BMNC	321	57.8	0.1 M $HClO_4$	[24]
Hollow IrCo	281	64.7	1 M $HClO_4$	[25]
IrCo nanospheres	284	56	0.5 M H_2SO_4	[26]
IrCo Nanodendrite	281	59.3	0.1 M $HClO_4$	[27]

Table S4. Comparison of overall water splitting activity data for bifunctional electrocatalysts.

Catalysts	electrolyte	η_{10}(mA cm^{-2})	Reference
Ir_1-CoP/CC	0.5 M H_2SO_4	1.61 V	This work
Ir_2-CoP/CC		1.56 V	
Ir_3-CoP/CC		1.50 V	
Ir_4-CoP/CC		1.50 V	
$Cu_{2-x}S@IrS_y$	0.1 M $HClO_4$	1.47 V	[28]
IrNi NCs	0.5 M H_2SO_4	1.58 V	[29]
CB[6]-Ir_2	0.05 M H_2SO_4	1.56 V	[30]
Ir/GF	0.5 M H_2SO_4	1.55 V	[18]
IrW ND	0.5 M H_2SO_4	1.48 V	[31]
Co-MoS_2-0.5	0.5 M H_2SO_4	1.9 V	[21]
Ir_6Ag_9NTs	0.5 M H_2SO_4	1.55 V	[32]
h-PNRO/C	0.1 M $HClO_4$	1.52 V	[33]
Ir NPs	0.5 M H_2SO_4	1.58 V	[34]
Ir nanowires	0.1 M $HClO_4$	1.62 V	[35]
ONPPGC/OCC	0.5 M H_2SO_4	1.66 V	[36]
$Ti_3C_2T_x$ MXene	0.1 M $HClO_4$	1.56 V	[37]
Ru_3Ni_3 NAs	0.5 M H_2SO_4	1.51 V	[38]

Reference

(1) Wu, J.; Wang, D.; Wan, S.; Liu, H.; Wang, C.; Wang, X. An Efficient Cobalt Phosphide Electrocatalyst Derived from Cobalt Phosphonate Complex for All-PH Hydrogen Evolution Reaction and Overall Water Splitting in Alkaline Solution. **2020**, *16* (15), 1900550.

(2) Yoon, H.; Song, H. J.; Ju, B.; Kim, D.-W. Cobalt Phosphide Nanoarrays with Crystalline-Amorphous Hybrid Phase for Hydrogen Production in Universal-PH. *Nano Res.* **2020**, *13* (9), 2469–2477.

(3) Ji, L.; Wang, J.; Teng, X.; Meyer, T. J.; Chen, Z. CoP Nanoframes as Bifunctional Electrocatalysts for Efficient Overall Water Splitting. *ACS Catal.* **2020**, *10* (1), 412–419.

(4) Wasalathanthri, R. N.; Jeffrey, S.; Awni, R. A.; Sun, K.; Giolando, D. M. Electrodeposited Copper–Cobalt–Phosphide: A Stable Bifunctional Catalyst for Both Hydrogen and Oxygen Evolution Reactions. *ACS Sustain. Chem. Eng.* **2019**, *7* (3), 3092–3100.

(5) Gao, W.; Yan, M.; Cheung, H.-Y.; Xia, Z.; Zhou, X.; Qin, Y.; Wong, C.-Y.; Ho, J. C.; Chang, C.-R.; Qu, Y. Modulating Electronic Structure of CoP Electrocatalysts towards Enhanced Hydrogen Evolution by Ce Chemical Doping in Both Acidic and Basic Media. *Nano Energy* **2017**, *38*, 290–296.

(6) Zhuang, M.; Ou, X.; Dou, Y.; Zhang, L.; Zhang, Q.; Wu, R.; Ding, Y.; Shao, M.; Luo, Z. Polymer-Embedded Fabrication of Co2P Nanoparticles Encapsulated in N,P-Doped Graphene for Hydrogen Generation. *Nano Lett.* **2016**, *16* (7), 4691–4698.

(7) Liu, S.; Liu, Q.; Lv, Y.; Chen, B.; Zhou, Q.; Wang, L.; Zheng, Q.; Che, C.; Chen, C. Ru Decorated with NiCoP: An Efficient and Durable Hydrogen Evolution Reaction Electrocatalyst in Both Acidic and Alkaline Conditions. *Chem. Commun.* **2017**, *53* (98), 13153–13156.

(8) Song, H.; Wu, M.; Tang, Z.; Tse, J. S.; Yang, B.; Lu, S. Single Atom Ru Doped CoP/CDs Nanosheets via Splicing of Carbon-Dots for Robust Hydrogen Production. *Angew. Chemie Int. Ed.* **2021**, *n/a* (n/a).

(9) Wu, J.; Han, N.; Ning, S.; Chen, T.; Zhu, C.; Pan, C.; Wu, H.; Pennycook, S. J.; Guan, C. Single-Atom Tungsten-Doped CoP Nanoarrays as a High-Efficiency PH-Universal Catalyst for Hydrogen Evolution Reaction. *ACS Sustain. Chem. Eng.* **2020**, *8* (39), 14825–14832.

(10) Tang, C.; Gan, L.; Zhang, R.; Lu, W.; Jiang, X.; Asiri, A. M.; Sun, X.; Wang, J.; Chen, L. Ternary FexCo1–XP Nanowire Array as a Robust Hydrogen Evolution Reaction Electrocatalyst with Pt-like Activity: Experimental and Theoretical Insight. *Nano Lett.* **2016**, *16* (10), 6617–6621.

(11) Huang, X.; Xu, X.; Li, C.; Wu, D.; Cheng, D.; Cao, D. Vertical CoP Nanoarray Wrapped by N,P-Doped Carbon for Hydrogen Evolution Reaction in Both Acidic and Alkaline Conditions. *Adv. Energy Mater.* **2019**, *9* (22), 1803970.

(12) Jiang, K.; Liu, B.; Luo, M.; Ning, S.; Peng, M.; Zhao, Y.; Lu, Y.-R.; Chan, T.-S.; de Groot, F. M. F.; Tan, Y. Single Platinum Atoms Embedded in Nanoporous Cobalt Selenide as Electrocatalyst for Accelerating Hydrogen Evolution Reaction. *Nat. Commun.* **2019**, *10* (1), 1743.

(13) Xiao, X.; Tao, L.; Li, M.; Lv, X.; Huang, D.; Jiang, X.; Pan, H.; Wang, M.; Shen, Y. Electronic Modulation of Transition Metal Phosphide via Doping as Efficient and PH-Universal Electrocatalysts for Hydrogen Evolution Reaction. *Chem. Sci.* **2018**, *9* (7), 1970–1975.

(14) Cao, B.; Cheng, Y.; Hu, M.; Jing, P.; Ma, Z.; Liu, B.; Gao, R.; Zhang, J. Efficient and Durable 3D Self-Supported Nitrogen-Doped Carbon-Coupled Nickel/Cobalt Phosphide Electrodes: Stoichiometric Ratio Regulated Phase- and Morphology-Dependent Overall Water Splitting Performance. *Adv. Funct. Mater.* **2019**, *29* (44), 1906316.

(15) Kim, J.; Shih, P.-C.; Qin, Y.; Al-Bardan, Z.; Sun, C.-J.; Yang, H. A Porous Pyrochlore Y2[Ru1.6Y0.4]O7–δ Electrocatalyst for Enhanced Performance towards the Oxygen Evolution Reaction in Acidic Media. *Angew. Chemie Int. Ed.* **2018**, *57* (42), 13877–13881.

(16) Cao, L.; Luo, Q.; Chen, J.; Wang, L.; Lin, Y.; Wang, H.; Liu, X.; Shen, X.; Zhang, W.; Liu, W.; Qi, Z.; Jiang, Z.; Yang, J.; Yao, T. Dynamic Oxygen

Adsorption on Single-Atomic Ruthenium Catalyst with High Performance for Acidic Oxygen Evolution Reaction. *Nat. Commun.* **2019**, *10* (1), 4849.

(17) Shang, C.; Cao, C.; Yu, D.; Yan, Y.; Lin, Y.; Li, H.; Zheng, T.; Yan, X.; Yu, W.; Zhou, S.; Zeng, J. Electron Correlations Engineer Catalytic Activity of Pyrochlore Iridates for Acidic Water Oxidation. *Adv. Mater.* **2019**, *31* (6), 1805104.

(18) Zhang, J.; Wang, G.; Liao, Z.; Zhang, P.; Wang, F.; Zhuang, X.; Zschech, E.; Feng, X. Iridium Nanoparticles Anchored on 3D Graphite Foam as a Bifunctional Electrocatalyst for Excellent Overall Water Splitting in Acidic Solution. *Nano Energy* **2017**, *40*, 27–33.

(19) Yin, J.; Jin, J.; Lu, M.; Huang, B.; Zhang, H.; Peng, Y.; Xi, P.; Yan, C.-H. Iridium Single Atoms Coupling with Oxygen Vacancies Boosts Oxygen Evolution Reaction in Acid Media. *J. Am. Chem. Soc.* **2020**, *142* (43), 18378–18386.

(20) Han, N.; Yang, K. R.; Lu, Z.; Li, Y.; Xu, W.; Gao, T.; Cai, Z.; Zhang, Y.; Batista, V. S.; Liu, W.; Sun, X. Nitrogen-Doped Tungsten Carbide Nanoarray as an Efficient Bifunctional Electrocatalyst for Water Splitting in Acid. *Nat. Commun.* **2018**, *9* (1), 924.

(21) Xiong, Q.; Zhang, X.; Wang, H.; Liu, G.; Wang, G.; Zhang, H.; Zhao, H. One-Step Synthesis of Cobalt-Doped MoS2 Nanosheets as Bifunctional Electrocatalysts for Overall Water Splitting under Both Acidic and Alkaline Conditions. *Chem. Commun.* **2018**, *54* (31), 3859–3862.

(22) Chen, H.; Shi, L.; Liang, X.; Wang, L.; Asefa, T.; Zou, X. Optimization of Active Sites via Crystal Phase, Composition, and Morphology for Efficient Low-Iridium Oxygen Evolution Catalysts. *Angew. Chemie Int. Ed.* **2020**, *59* (44), 19654–19658.

(23) Park, J.; Choi, S.; Oh, A.; Jin, H.; Joo, J.; Baik, H.; Lee, K. Hemi-Core@frame AuCu@IrNi Nanocrystals as Active and Durable Bifunctional Catalysts for the Water Splitting Reaction in Acidic Media. **2019**, *4* (3), 727–734.

(24) Chen, X.; Xu, M.; Li, S.; Li, C.; Sun, X.; Mu, S.; Yu, J. Ultrafine IrNi Bimetals

Encapsulated in Zeolitic Imidazolate Frameworks-Derived Porous N-Doped Carbon for Boosting Oxygen Evolution in Both Alkaline and Acidic Electrolytes. *Adv. Mater. Interfaces* **2020**, *7* (24), 2001145.

(25) Li, Y.; Xing, L.; Yu, D.; Libanori, A.; Yang, K.; Sun, J.; Nashalian, A.; Zhu, Z.; Ma, Z.; Zhai, Y.; Chen, J. Hollow IrCo Nanoparticles for High-Performance Overall Water Splitting in an Acidic Medium. *ACS Appl. Nano Mater.* **2020**, *3* (12), 11916–11922.

(26) Zhu, J.; Wei, M.; Meng, Q.; Chen, Z.; Fan, Y.; Hasan, S. W.; Zhang, X.; Lyu, D.; Tian, Z. Q.; Shen, P. K. Ultrathin-Shell IrCo Hollow Nanospheres as Highly Efficient Electrocatalysts towards the Oxygen Evolution Reaction in Acidic Media. *Nanoscale* **2020**, *12* (47), 24070–24078.

(27) Fu, L.; Zeng, X.; Cheng, G.; Luo, W. IrCo Nanodendrite as an Efficient Bifunctional Electrocatalyst for Overall Water Splitting under Acidic Conditions. *ACS Appl. Mater. Interfaces* **2018**, *10* (30), 24993–24998.

(28) Joo, J.; Jin, H.; Oh, A.; Kim, B.; Lee, J.; Baik, H.; Joo, S. H.; Lee, K. An IrRu Alloy Nanocactus on Cu2−xS@IrSy as a Highly Efficient Bifunctional Electrocatalyst toward Overall Water Splitting in Acidic Electrolytes. *J. Mater. Chem. A* **2018**, *6* (33), 16130–16138.

(29) Pi, Y.; Shao, Q.; Wang, P.; Guo, J.; Huang, X. General Formation of Monodisperse IrM (M = Ni, Co, Fe) Bimetallic Nanoclusters as Bifunctional Electrocatalysts for Acidic Overall Water Splitting. *Adv. Funct. Mater.* **2017**, *27* (27), 1700886.

(30) You, H.; Wu, D.; Chen, Z.; Sun, F.; Zhang, H.; Chen, Z.; Cao, M.; Zhuang, W.; Cao, R. Highly Active and Stable Water Splitting in Acidic Media Using a Bifunctional Iridium/Cucurbit[6]Uril Catalyst. *ACS Energy Lett.* **2019**, *4* (6), 1301–1307.

(31) Lv, F.; Feng, J.; Wang, K.; Dou, Z.; Zhang, W.; Zhou, J.; Yang, C.; Luo, M.; Yang, Y.; Li, Y.; Gao, P.; Guo, S. Iridium–Tungsten Alloy Nanodendrites as PH-Universal Water-Splitting Electrocatalysts. *ACS Cent. Sci.* **2018**, *4* (9), 1244–1252.

(32) Zhu, M.; Shao, Q.; Qian, Y.; Huang, X. Superior Overall Water Splitting Electrocatalysis in Acidic Conditions Enabled by Bimetallic Ir-Ag Nanotubes. *Nano Energy* **2019**, *56*, 330–337.

(33) Oh, A.; Kim, H. Y.; Baik, H.; Kim, B.; Chaudhari, N. K.; Joo, S. H.; Lee, K. Topotactic Transformations in an Icosahedral Nanocrystal to Form Efficient Water-Splitting Catalysts. *Adv. Mater.* **2019**, *31* (1), 1805546.

(34) Fu, L.; Zeng, X.; Huang, C.; Cai, P.; Cheng, G.; Luo, W. Ultrasmall Ir Nanoparticles for Efficient Acidic Electrochemical Water Splitting. *Inorg. Chem. Front.* **2018**, *5* (5), 1121–1125.

(35) Fu, L.; Yang, F.; Cheng, G.; Luo, W. Ultrathin Ir Nanowires as High-Performance Electrocatalysts for Efficient Water Splitting in Acidic Media. *Nanoscale* **2018**, *10* (4), 1892–1897.

(36) Lai, J.; Li, S.; Wu, F.; Saqib, M.; Luque, R.; Xu, G. Unprecedented Metal-Free 3D Porous Carbonaceous Electrodes for Full Water Splitting. *Energy Environ. Sci.* **2016**, *9* (4), 1210–1214.

(37) Peng, X.; Zhao, S.; Mi, Y.; Han, L.; Liu, X.; Qi, D.; Sun, J.; Liu, Y.; Bao, H.; Zhuo, L.; Xin, H. L.; Luo, J.; Sun, X. Trifunctional Single-Atomic Ru Sites Enable Efficient Overall Water Splitting and Oxygen Reduction in Acidic Media. **2020**, *16* (33), 2002888.

(38) Yang, J.; Shao, Q.; Huang, B.; Sun, M.; Huang, X. PH-Universal Water Splitting Catalyst: Ru-Ni Nanosheet Assemblies. **2019**, *11*, 492–504.